

## **Electronic Supplementary Information**

# **Multifunctional Flexible Carbon Aerogels based on Sustainable Bacterial Cellulose**

Seeni Meera Kamal Mohamed,<sup>a,\*</sup> Benjamin Ignatzi,<sup>a</sup> Rebekka Probst,<sup>a</sup> Beruktayet Fekadu,<sup>b</sup> Max Zinke,<sup>a</sup> Lennart Barth,<sup>a</sup> Marina Schwan,<sup>a</sup> Marion Bartsch,<sup>b</sup> Barbara Milow<sup>a</sup>

<sup>a</sup>*Department of Aerogels and Highly Porous Materials and <sup>b</sup>Department of Digitally Integrated Microstructure and Mechanics, Institute for Frontier Materials on Earth and in Space, German Aerospace Center (DLR), Cologne, Germany.*

*E-mail: [seenimeera.kamalmohamed@dlr.de](mailto:seenimeera.kamalmohamed@dlr.de)*

### **1. Experimental Section:**

#### **1.1. Raw Material and Reagents:**

The bacterial cellulose (BC) was obtained as cubes (1 x 1 x 1 cm<sup>3</sup>) from a local store, which is a trademark product from Chaokoh, Thailand. The reagents, resorcinol (98%) and sodium carbonate (anhydrous, 99.8%) were purchased from Sigma Aldrich, Germany. Formaldehyde (23.5%), low methanol solution was procured from Carl Roth, Germany. Sodium hydroxide and ethanol (99.5%) was procured from Th. Geyer, Germany. Deionized water was used throughout the experiments. All the reagents were used as received without any further purification except BC cubes.

#### **1.2. Purification of BC Cubes:**

The BC cubes were obtained in food graded state which contains sugar components. These adsorbed sugar components were removed by washing as follows: first washed several times with deionized water and treated with 0.1M NaOH solution for 48 hours under stirring followed by washing with water until neutral pH obtained. The washed BC cubes were used for further experiments.

#### **1.3. Preparation of BC, BC-Resorcinol-Formaldehyde (BC-RF) and *f*-RF Aerogels:**

The washed BC cubes' (hydrogel) solvent was exchanged with ethanol followed by super-critical drying to obtain pristine BC aerogels, labelled as BC-A. Further, RF solution was prepared using the following recipe reported by Schwan *et al.*<sup>1</sup> The molar ratios, R/C: 50, R/W:

0.008, R/F: 0.5 at pH: 5.43 - 5.65. The washed BC cubes were immersed in the RF solution under ultrasonication to achieve good infiltration. RF infiltrated BC cubes were placed in a container in an oven at 80 °C for 1 week for gelation. After the gelation, BC-RF cubes were washed and solvent exchanged with ethanol for super-critical drying to achieve dried aerogels and labelled as BC-RF-A. The schematic of the BC-A, and BC-RF-A preparation is presented in Fig. S1. As a control, *f*-RF aerogel was prepared as per the recipe reported above and labelled as *f*-RF-A.

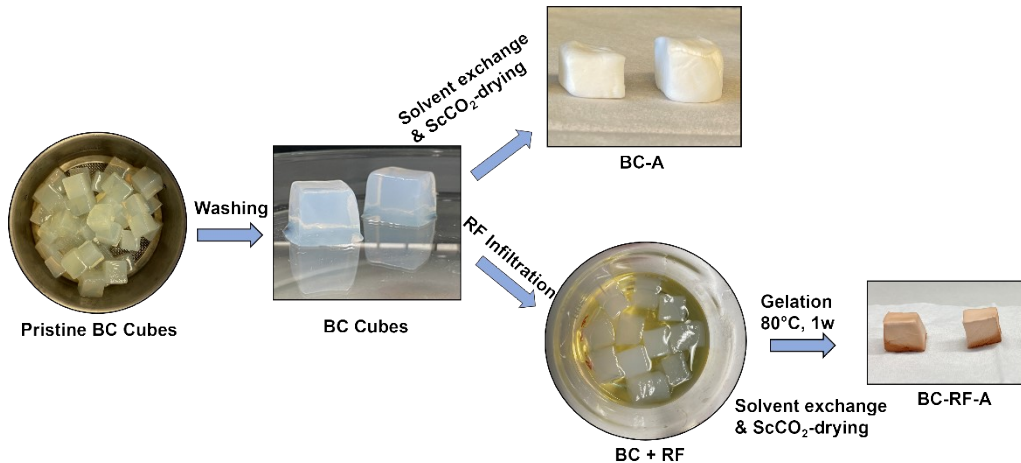


**Fig. S1:** Schematic representation of BC-A and BC-RF-A preparation.

#### 1.4. Preparation of BC-RF Carbon Aerogels (BC-RF-C-A):

The super-critically dried BC and BC-RF aerogels were pyrolyzed under the following conditions: (i) 20-500 °C, 300 K/h, 1 h dwell at 500 °C & (ii) 500-1000 °C, 600 K/h, 2 h dwell at 1000 °C in an Ar (static) environment and further cool down to room temperature. The carbonization was carried out in a tube furnace ( $\phi = 150$  mm,  $l = 500$  mm, Gero Hochtemperaturöfen GmbH, Germany), and the schematic diagram of the oven used in pyrolysis is presented in Fig. S2. The samples were placed in the oven as described in Fig S2, and the atmosphere was supplied with Argon for 4 times in a cycle followed by vacuum (50 mbar) in-order to remove the Oxygen before the beginning of the pyrolysis process, and the vacuum (50 mbar) is maintained until end of the cooling to room temperature. The pyrolysis was performed using square bowls (BCR) made of Alumina dense (AL99-G) (99.7%  $\text{Al}_2\text{O}_3$ ) from Gieß-Technische-Sonderkeramik GmbH & Co. KG, Germany. The pristine BC-A showed high shrinkage, and almost nothing is present at the end of the pyrolysis (very low carbon yield is obtained in some cases), whereas RF infiltrated BC exhibited low shrinkage. In the current study, sample dimension, sample amount and type of gas flow (static) and doping (RF infiltration amount) decides the carbon yield. We have performed the pyrolysis in a static Ar

atmosphere using pristine BC cubes of small dimensions ( $1 \text{ cm}^3$ ). This is probably the reason why the pristine BC aerogels failed to survive the carbonization in most cases (in some cases low carbon yield is obtained). However, the infiltration of RF into BC survived the carbonization with minimal shrinkage. The pyrolysis process of BC-RF-A to BC-RF-C-A is depicted in Fig. S3. Moreover, *f*-RF-A was also pyrolyzed to form its carbon aerogel as a control and labelled as *f*-RF-C-A.

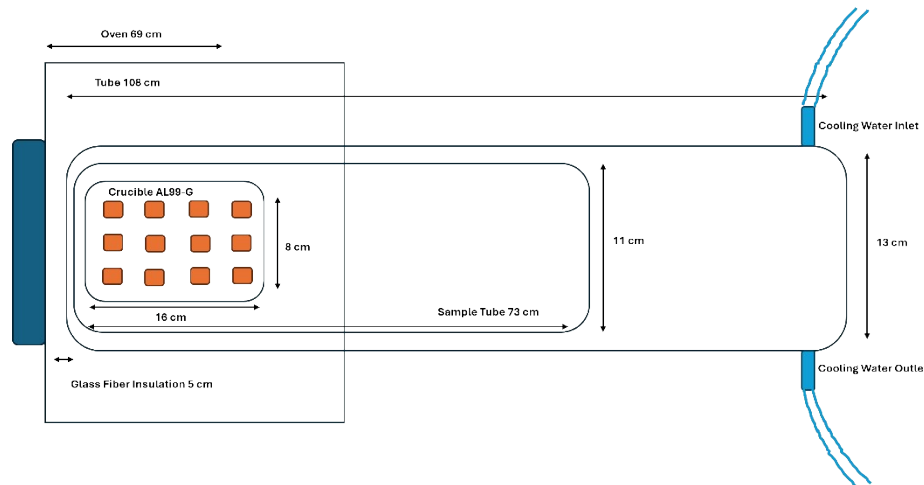


**Fig S2:** Schematic diagram of the oven used for pyrolysis (top view with sample arrangement is shown).

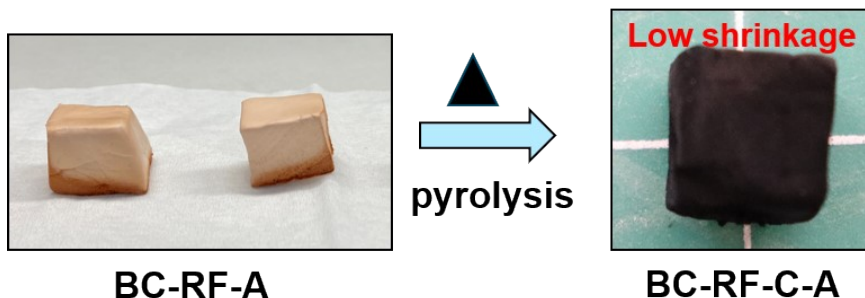


**Fig. S3:** Pyrolysis of BC-RF-A to BC-RF-C-A

### 1.5. Characterization Methods:

The gelation of the *f*-RF and BC-RF was carried out in an oven (Memmert Universal Oven UF110) at 80 °C. The super-critical drying of all the alcogels was performed using super-critical CO<sub>2</sub> drying technique at 115 bar and 60 °C. The skeletal densities ( $\rho_s$ ) of the aerogels were analyzed using AccuPyc II 1340 Helium Pycnometer from Micromeritics, Germany. The purge- and cycle fill pressure was set to 19.500 psig and a pressure change rate of <0.0050 psig/min was set as an equilibrium condition and the samples were purged 10 times. The bulk densities ( $\rho_b$ ) of the aerogels were analyzed using GeoPyc 1360 Sand Pycnometer from

Micromeritics, Germany. The skeletal and bulk densities of the samples were average of 10 cycle measurements for each sample. The porosities of the prepared aerogels were calculated using the formula,  $P = (1 - (\rho_b / \rho_s)) * 100$ . The physisorption measurements in-order to determine the surface area, pore volume, and pore size of the aerogels were carried out using  $N_2$  adsorption/desorption isotherm analysis. The analysis was performed using a MicroActive 3Flex 3500 Gas Sorption Analyzer from Micromeritics at a temperature of 77.3 K with a relative pressure ( $P/P_0$ ) range of 0.01-1.0. The samples were pretreated with Smart VacPrep 067 HIVAC at 120 °C for 12 h (except carbon samples) and 200 °C for 12 h (for carbon samples) before starting the measurements. The specific surface areas were calculated using Brunauer-Emmett-Teller (BET) method, and the C-value was positive. The pore size distribution (PSD) curves were obtained using the Barrett-Joyner-Halenda (BJH) method. The total pore volume ( $V_p$ ) was estimated from the adsorption branches of the isotherm at relative pressure ( $P/P_0$ ) of 0.995. The pore sizes ( $D_p$ ) were obtained from the maxima in the BJH pore size distribution curves. The pore size distributions of the carbon aerogels were obtained using DFT method (Geometry: slit and Model:  $N_2$  - DFT model). The application of BET method to microporous materials followed the recommendation by IUPAC.<sup>3</sup>  $CO_2$  adsorption capacities of flexible carbon aerogels were derived from  $CO_2$  sorption isotherms which were measured using a TriStar II 3020 physisorption analyzer (Micromeritics GmbH, Germany) at 273 and 298 K. The relative pressure was increased in  $\Delta p/p_0 = 0.00050$  steps until a final relative pressure of  $p/p_0 = 0.030$  for measurements at 273 K and in  $\Delta p/p_0 = 0.00025$  steps until a final relative pressure of  $p/p_0 = 0.016$  for measurements at 298 K. Before the measurements, flexible carbon aerogels were outgassed under vacuum conditions ( $2.67 \cdot 10^{-3}$  kPa) at 200 °C for 12 h using a Smart VacPrep 067 HIVAC device (Micromeritics GmbH, Germany). The  $N_2$  and  $CO_2$  sorption isotherms were measured for all the samples in triplicate. The mechanical stress-strain behavior of the flexible carbon aerogels (BC-RF-C-A) was characterized by cyclic compression tests. The results are provided for a cubic aerogel sample (Dimension: cross section 10.5 mm x 11.5 mm, height 9.5 mm) which was compressed using an Instron 5543A universal testing machine with a 50 N load cell at a displacement rate of 10 mm/min during loading and unloading for 100 cycles with reaching a maximum compressive strain of 80% in each cycle. Infrared spectra of different aerogels were recorded using a Fourier transform infrared (FT-IR) spectrometer, Bruker-Tensor 27 instrument with a resolution of 16  $cm^{-1}$  and 100 scans over the range of 400-4000  $cm^{-1}$  by making them as pellets using KBr. The Raman spectra of the flexible carbon aerogels were analyzed by Raman Spectroscopy (HORIBA: XploRA Plus) using a laser excitation wavelength of 532 nm diode pumped solid state laser (DPSS) with an excitation

power of 25 mW and operated at 1% laser power. The spectra were normalized to 100 and the peaks D1, D2, and G were fitted using Lorenz fitting. The thermal stability of the samples was analyzed using thermo gravimetric analyses (TGA). TGA of the samples were performed using Simultaneous Thermal Analyzer (Model: STA 449 F3 Jupiter) from NETZSCH-Gerätebau GmbH, Germany. The measurements were performed under an Ar atmosphere with a heating rate of 10 K/min for the temperature range 40 - 800 °C. Wide angle X-ray scattering (WAXS) measurements were attained using Bruker D8 Advance with a Cu K $\alpha$  radiation ( $\lambda = 1.5406 \text{ \AA}$ ) at 35 kV and 30 mA. The Goniometer has a radius of 280 mm. The detector is a LynxEExe XET from Bruker. The conditions for the measurements are: (i) scanning ranges from 10 - 100° of 2 $\theta$  with a step size of 0.01° and the time/step was 3 s; (ii) primary slit: fixed divergence slit with 0.22° to illuminate the sample, secondary slit: 5.232 mm (full opened), detector opening: 2.305°. The mathematical detector slit is 0.012° for the resolution and the primary and secondary Soller-slit is 2.5°. The samples were dry grinded to a suitable size with a mortar and pestle. The powder was pressed manually into a small cavity in a single crystal with 5 mm diameter. The single crystal is a low background-holder for small amounts of powder and provide no peaks in the measured 2 $\theta$  range. The size and morphology of the different aerogels were analyzed using a ZEISS ULTRA55 scanning electron (SEM) (Zeiss SMT, Oberkochen, Germany) with a low operating voltage of 2-3 kV. All the samples were sputtered using a thin layer of platinum using BAL-TEC SCD 500 Sputter Coater with a current of 21 mA for 60 s. The oil absorption efficiency of the flexible carbon (BC-RF-C-A) aerogel (% weight gain) is calculated using the formula,  $(\text{weight after saturated absorption} - \text{initial weight}) / \text{initial weight} * 100$ .<sup>2</sup>

## 2. Results and Discussion:

### Scanning electron microscopy

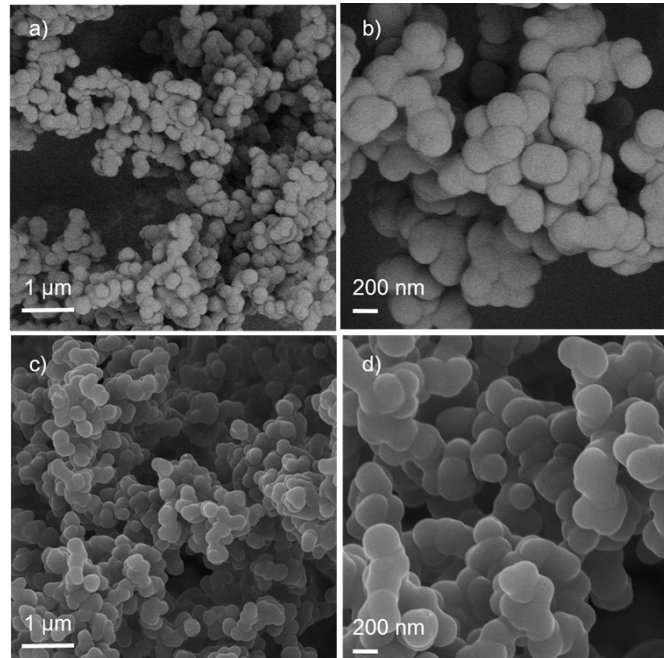


**Fig. S4:** SEM images of *f*-RF-A (a & b) and *f*-RF-C-A (c & d).

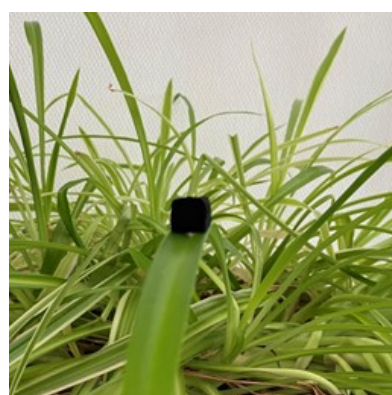


**Fig. S5:** Ultralight BC-RF-C-A standing on the leaf of spider plant.

## N<sub>2</sub> Physisorption Isotherm

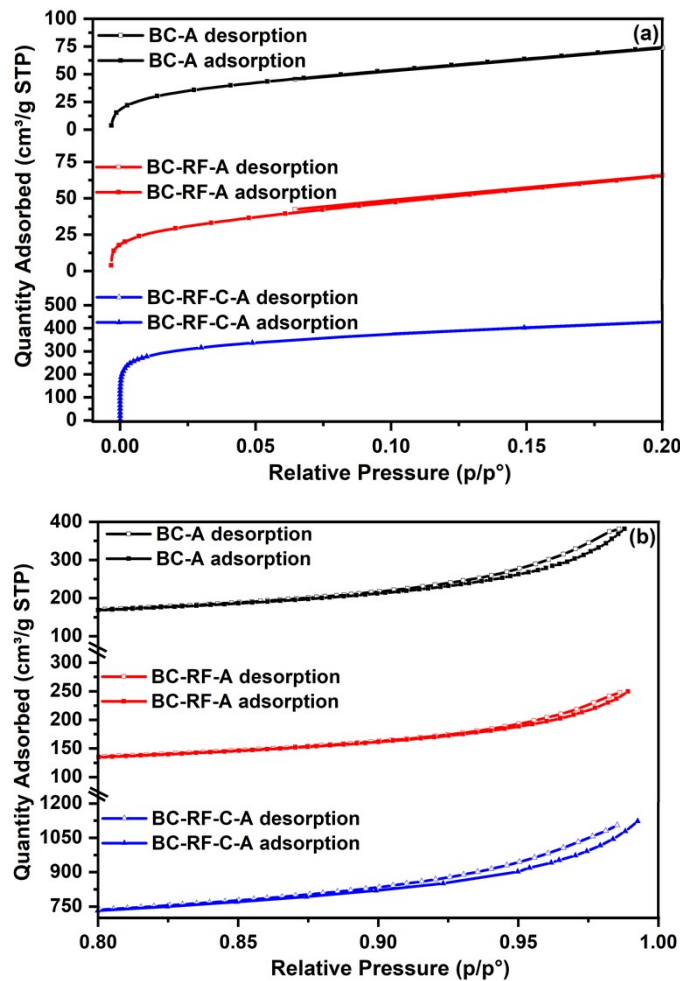


**Fig. S6:** Expanded regions of N<sub>2</sub> adsorption/desorption isotherm of the prepared different aerogels: (a) lower p/p<sub>0</sub> region and (b) higher p/p<sub>0</sub> region.

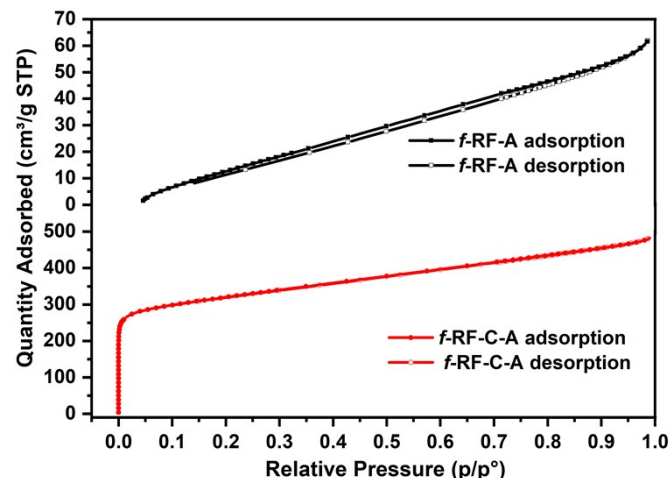


**Fig. S7:** N<sub>2</sub> adsorption/desorption isotherm of f-RF-A and f-RF-C-A.

### Pore size distribution graph

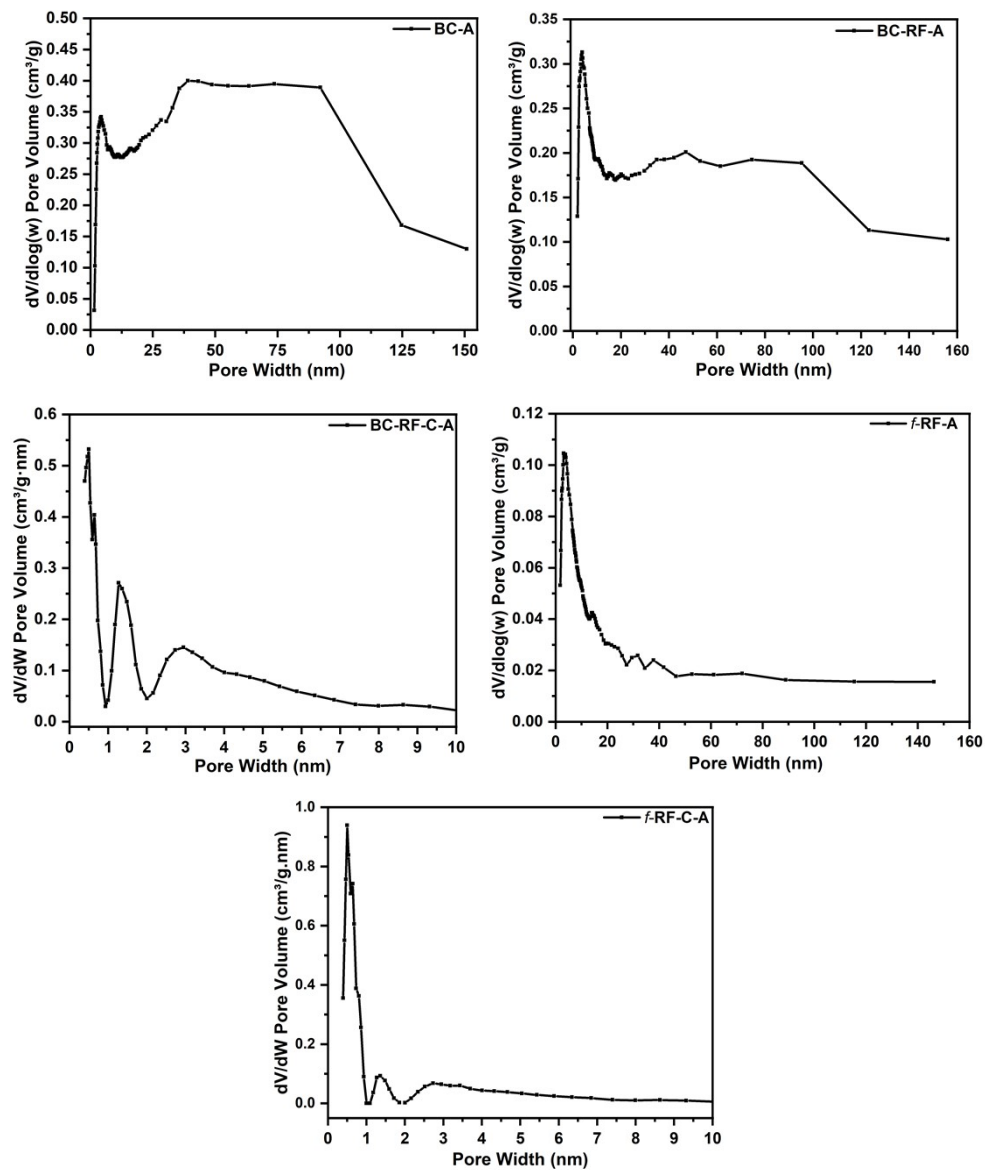


**Fig. S8:** Pore size distribution graphs of different aerogels calculated using BJH (BC-A, BC-RF-A & *f*-RF-A) and DFT (*f*-RF-C-A & BC-RF-C-A) calculation.

### Thermo gravimetric analyses (TGA)

The thermal stabilities of the pristine aerogels were measured using thermo gravimetric analysis and presented in Fig. S9. BC-A exhibit a weight loss of 4.42% until 100 °C because of the dehydration (removal of moisture and water). The weight loss between 210 and 430 °C is due to the depolymerization, and pyrolytic decomposition (oxidation) of the organic phase present in the BC leads to the production of gaseous products.<sup>4,5</sup> The gaseous products include  $\text{H}_2\text{O}$ ,  $\text{CO}_2$  and other volatile compounds. The final (carbon) residue at 600 °C is found to be 7.21%. The carbonization of cellulose and cellulose depolymerization often results in lower carbonization yield. Jiamsawat *et al.*<sup>6</sup> reported a carbonization of yield of 2.8% for pure

bacterial cellulose mates. Padmanabhan *et al.*<sup>7</sup> obtained a weight loss of 95% between 100 and 500 °C and final residue is found to be 5% for BC. The sample, *f*-RF-A exhibit a weight loss up to 100 °C due to the removal of water and moisture at a loss of 3.56%. The weight loss continues to occur between 100 and 270 °C due to the removal of unreacted organics and hydroxyl groups at a loss of 4.17%. The major degradation occurs between 270 and 600 °C due to the removal of major organics present in the RF polymeric backbone with a weight loss of 29.07%. The weight loss continues further and the residue is obtained as 54.43% at 800 °C. TGA curve of BC-*f*-RF-A appears as a blend of BC and *f*-RF-A. The initial degradation up to 100 °C resulted in a weight loss of 2.16% due to the removal of water and moisture present in the aerogels. The major decomposition occurs between 100 to 400 °C because of the removal and decomposition of major organics present in the samples. The weight loss in this region is found to be 43.32% and the weight loss continues until 800 °C. The carbon residue present at 800 °C is amounted to 31.78%. TGA curves of the pristine aerogel samples clearly provide the degradation pattern and their thermal stability upon thermal treatment under an inert atmosphere. Moreover, TGA profile of BC-*f*-RF-A indicates that the infiltration of RF into BC network improved the residue yield from 7.21 to 31.78%.

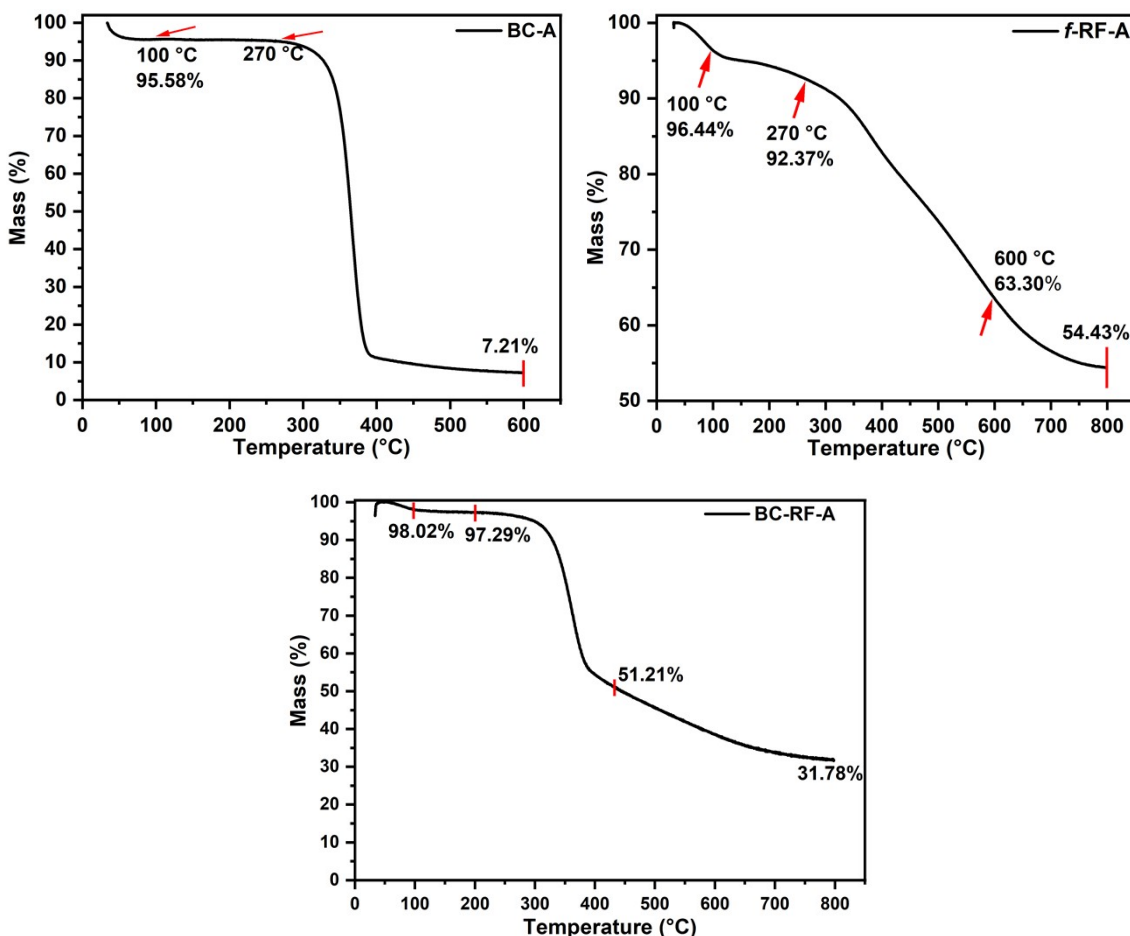


**Fig. S9:** TGA graphs of BC-A, *f*-RF-A, and BC-*f*-RF-A.

## CO<sub>2</sub> adsorption isotherm

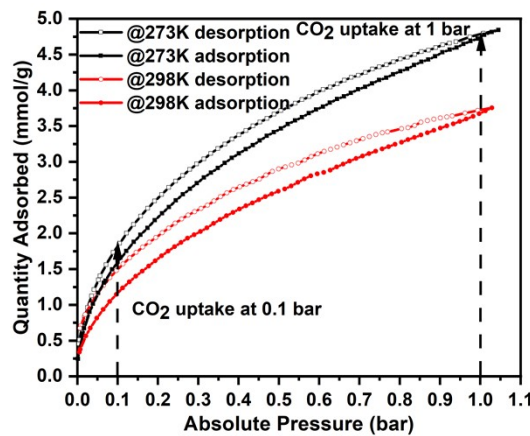


**Fig. S10:** CO<sub>2</sub> adsorption isotherm of f-RF-C-A at two different temperatures.

## FT-IR Spectra

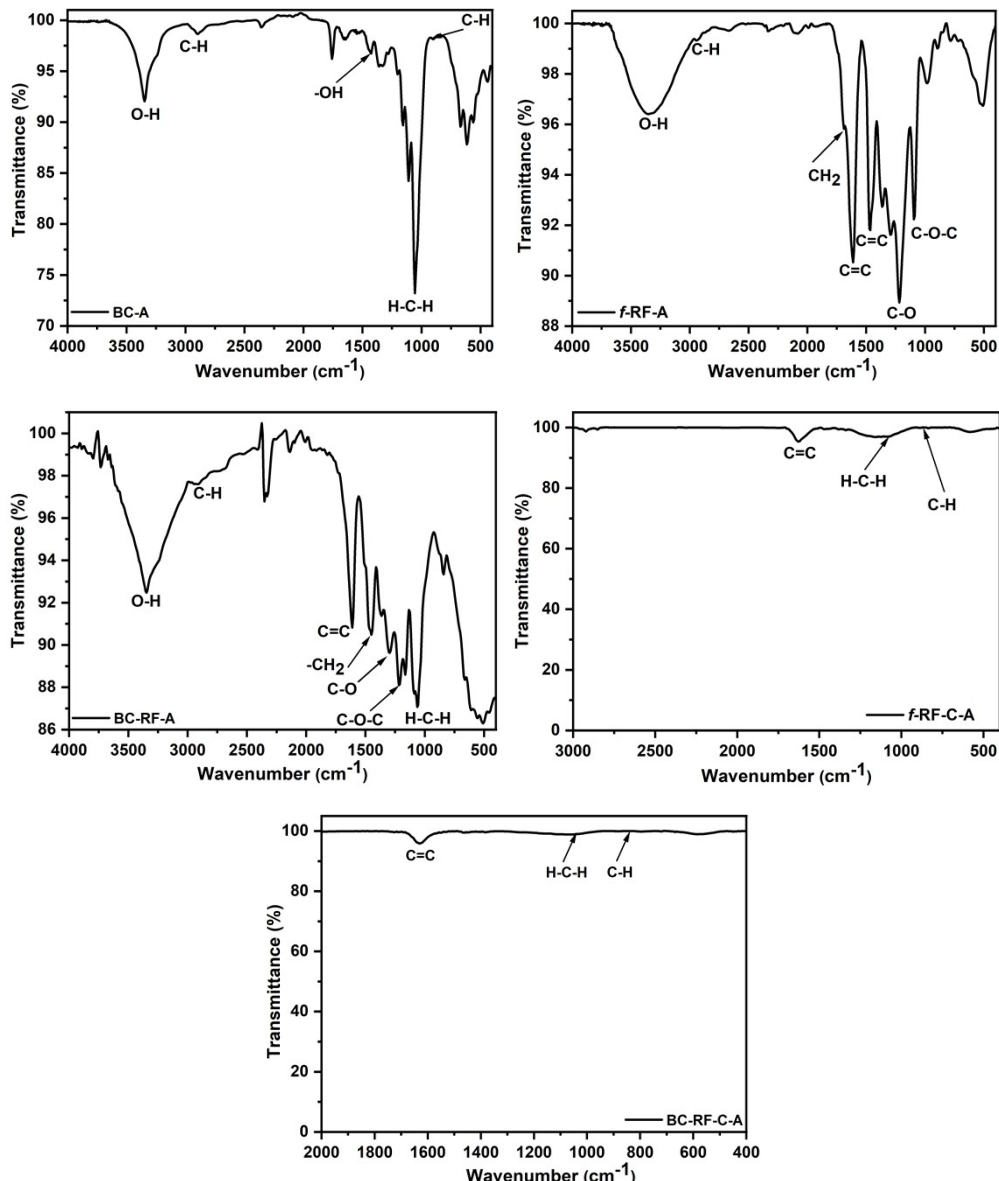


**Fig. S11:** FT-IR spectra of produced different aerogels.

### X-ray diffraction pattern

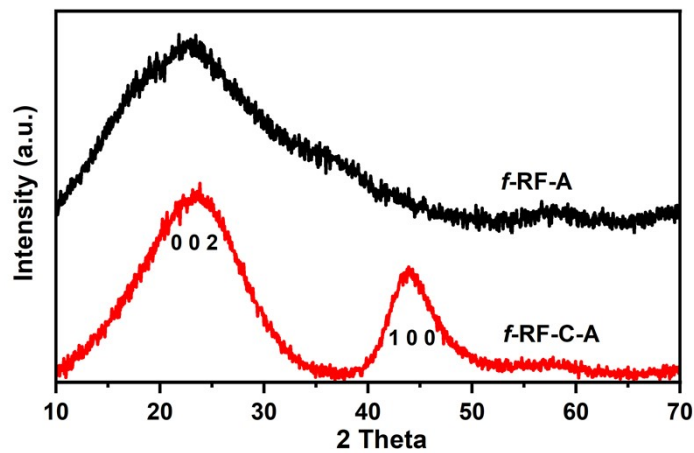


**Fig. S12:** X-ray diffraction pattern of *f*-RF-A and *f*-RF-C-A.

### Scanning electron microscope images

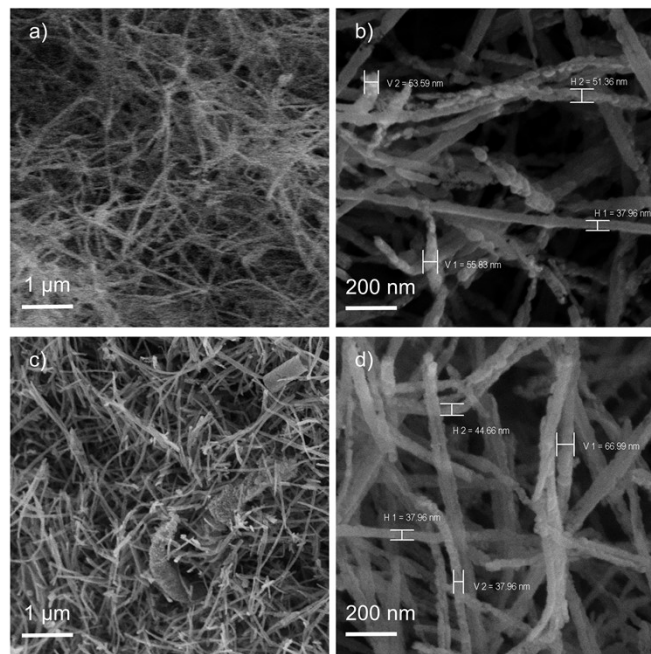


**Fig. S13:** SEM images of flexible carbon aerogels (BC-RF-C-A) after cyclic compression test (a & b) after 1 cycle and (c & d) after 100 cycles.

### Contact angle measurements

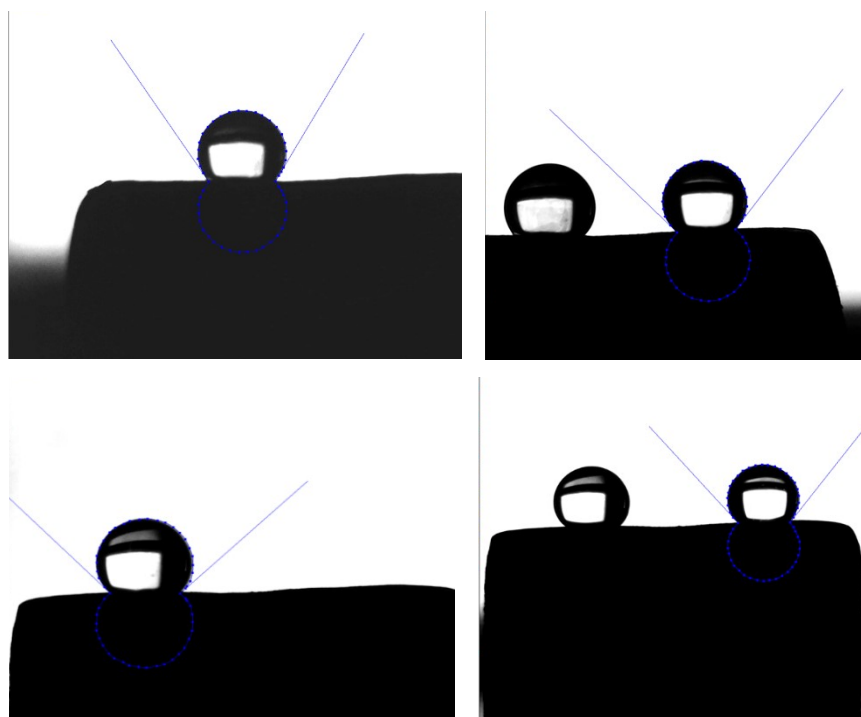


**Fig. S14:** The measurement of water contact angle for flexible carbon aerogel (BC-RF-C-A).

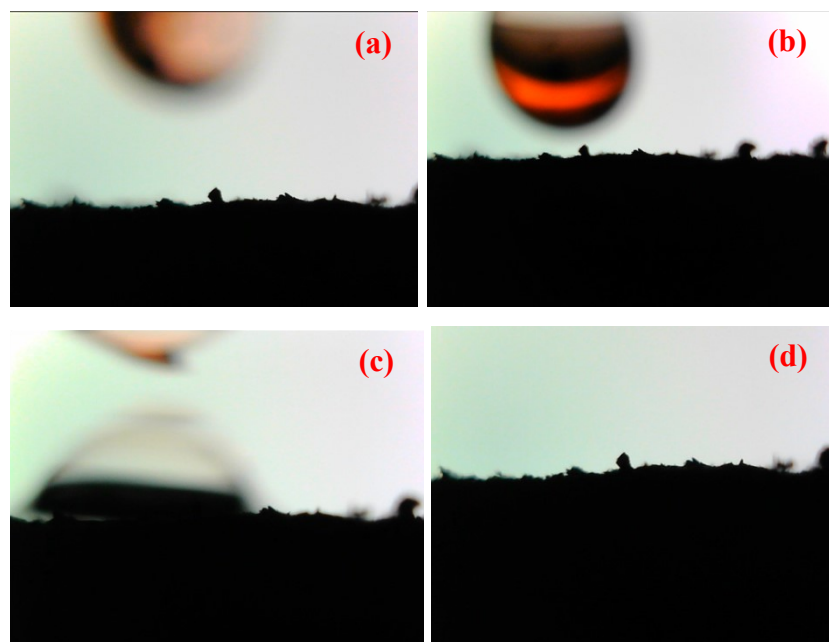


**Fig. S15:** Process of cyclohexane droplet absorption (a-d) and the measurement of contact angle with cyclohexane (d) over flexible carbon aerogel (BC-RF-C-A).

## Oil absorption tests



**Fig. S16:** (a) Artificial seawater (3.5% NaCl) & (b) Cyclohexane dyed with Sudan III.

**Table S1:** Water contact angle measurements of flexible carbon aerogel (BC-RF-C-A).

Trials	Contact Angle		Average (°)	Final contact angle (°)
	Right Side	Left Side		
Trial 1	124.35	121.42	122.88	
Trial 2	132.97	130.51	131.74	
Trial 3	137.20	138.17	137.68	130.71 ± 5.26
Trial 4	131.90	129.18	130.54	

## List of videos:

**Video S1:** Video of the cyclic compression test.

**Video S2:** Video of the water contact angle test.

**Video S3:** Video of the oil (cyclohexane) absorption test.

**Video S4.** Video of the flame retardancy test.

## References:

1. M. Schwan and L. Ratke, *J. Mater. Chem., A*, 2013, **1**, 13462-13468.
2. Z-Y. Wu, C. Li, H-W. Liang, Y-N. Zhang, X. Wang, J-F. Chen, S-H. Yu, *Sci. Rep.*, 2014, **4**, 4079.
3. M. Thommes, K. Kaneko, A. V. Neimark, J. P. Olivier, F. Rodriguez-Reinoso, J. Rouquerol, K. S.W. Sing, *Pure Appl. Chem.*, 2015, **87**, 1051-1069.
4. R. L. Oliveira, J. G. Vieira, H. S. Barud, R. M. N. Assunção, G. R. Filho, S. J. L. Ribeiroa, Y. Messadeqqa, *J. Braz. Chem. Soc.*, 2015, **26**(9) 1861-1870.
5. H. H. M. Nguyen, K. V. M. Tan, T. T. T. Van, H. N. Nguyen, A. N. Q. Phan, A. T. T. Tran, P. K. Le1, K. A. Le, K. D. Nguyen, H. V. Le, *J. Porous Mater.*, 2023, **30**, 1195–1205.
6. C. Jiamsawat, T. Wasanapiarnpong, K. Srikulkit, *Mater. Today Commun.*, 2022, **33**, 104382.
7. S. K. Padmanabhan, C. Protopapa, A. Licciulli, *Process Biochem.*, 2021, **103**, 31-38.